



Punching strength of RC slabs with asymmetric point loads

Maurício de Pina Ferreira*, Paulo Víctor Prazeres Sacramento, Aarão Ferreira Lima Neto, Marcelo Rassy Teixeira and Dênio Ramam Carvalho de Oliveira

Faculdade de Engenharia Civil, Universidade Federal do Pará, Rua Augusto Corrêa, 1, 66075-900, Cx. Postal 8619, Belém, Pará, Brazil. *Author for correspondence. E-mail: mpina@ufpa.br

ABSTRACT. This paper presents results of tests on 18 one-way reinforced concrete slabs under point loads having as main variable the transverse flexural reinforcement ratio, the loading position and the width of the slab. The response of the slabs is described and discussed in terms of deflections, strains of the concrete and of rebars, cracking pattern, failure modes and failure loads. Experimental results are also used to discuss and evaluate theoretical treatments presented by American Concrete Institute 318 (ACI, 2014) and Eurocode 2 (Comité Européen de Normalisation [CEN], 2005). All slabs failed by punching shear and results indicate that the recommendations presented by the codes are conservative, especially those related to the prediction of one-way shear resistance of reinforced concrete flat slabs.

Keywords: one-way slabs, punching, shear, asymmetric loading.

Resistência à punção de lajes de concreto armado com cargas concentradas assimétricas

RESUMO. Este trabalho apresenta resultados de ensaios em 18 lajes unidirecionais de concreto armado sob carregamento concentrado, tendo como variáveis a taxa de armadura de flexão transversal, a posição de carregamento e a largura da laje. Seu comportamento é descrito e discutido em termos de deslocamentos, deformações do concreto e das armaduras, padrão de fissuração, modos e cargas de ruptura. Os resultados experimentais também são usados para discutir e avaliar as recomendações apresentados pelas normas ACI 318 (2014) e Eurocode 2 (CEN, 2005). Todas as lajes romperam por punção e os resultados indicam que as recomendações normativas são relativamente conservadoras, especialmente aquelas relacionadas com a previsão da resistência ao cisalhamento unidirecional de lajes lisas de concreto armado.

Palavras-chave: lajes unidirecionais, punção, cisalhamento, carregamento assimétrico.

Introduction

There are a number of design situations in which reinforced concrete slabs are submitted to asymmetric concentrated loads distributed on small areas. This can occur in the case of flat slabs, in composite concrete and steel structures and in precast concrete buildings, as show in Figure 1a. It may also occur in the case of slab bridges supported on bearing pads or submitted to several moving loads caused by the wheels of heavy vehicles, as shown in Figures 1b and c. Their shear resistance is usually checked considering two critical cases: slab failing by diagonal tension along its full width with a behavior similar to beams (see Figure 2a); slab failing by punching shear, which is characterized by a truncated conical or pyramidal failure surface around the loaded area (see Figure 2b).

Regan and Rezai-Jorabi (1988) point out that in the first case, it is assumed a constant shear distribution along the width of the slab, and that for punching shear, it is considered a polar-symmetric distribution of shear. Lantsoght, van der Veen, Walraven, and Joost (2013) emphasizes that there is little experimental evidence available for the case of one-way slabs under concentrated loads close to the support, contrasting with the fact that the first tests date from the early 20th century (Forsell & Holmberg, 1946). This paper presents results of 18 tests on one-way reinforced concrete slabs submitted to point loads, in which were varied the loading position (a), the slabs' width and the flexural reinforcement ratio in the transverse direction (ρ_y). Observed ultimate loads and failure modes are presented and compared to those theoretically predicted by ACI 318 (2014) and Eurocode 2 (CEN, 2005).

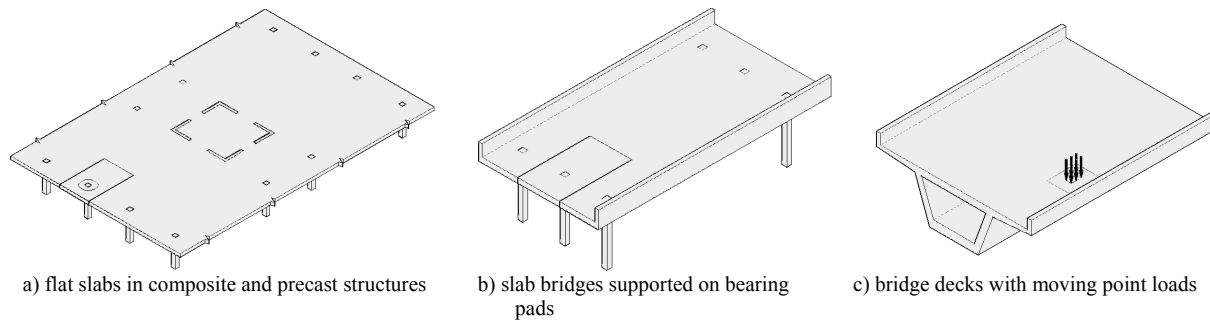


Figure 1. Practical examples of concrete slabs with asymmetric point loads.

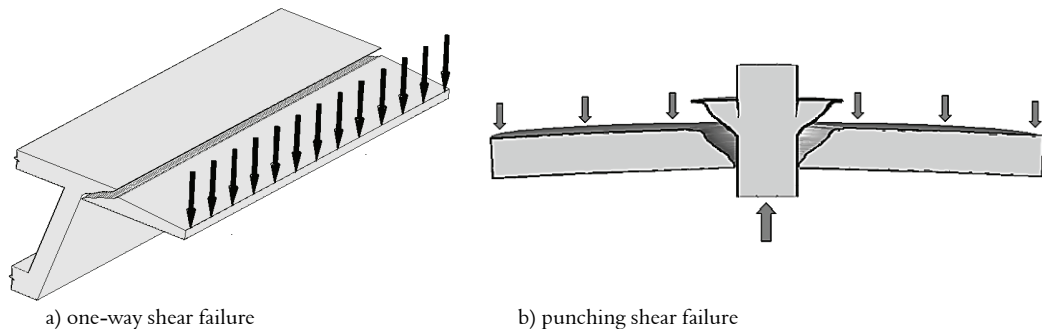


Figure 2. Shear failure of reinforced concrete slabs.

Material and methods

Experimental program

Experimental tests were carried on eighteen one-way reinforced concrete slabs, where twelve were square slabs with sides of 1.8 m and 110 mm thick and six were rectangular slabs with 1.8 m length, widths of 1.0 and 1.4 m and with thickness varying between 115 to 135 mm. The effect of asymmetry was evaluated as a function of both loading position (a) and flexural reinforcement ratio in the transverse direction (ρ_y). The distance of the loading position to the slabs' center (a) varied from 0, 267, 400 and 480 mm.

Samples from the steel bars used as flexural reinforcement were submitted to tensile tests. The profile of their stress-strain curves showed a linear-elastic response before yielding, with a well-defined yield plateau. In the longitudinal direction the flexural reinforcement was constant and had 12.5 mm bars with $f_y = 515$ MPa and $E_s = 213$ GPa at spacings of 99 mm, anchored in their ends by 180° hooks. In the transverse direction, the flexural reinforcement varied, and were used: 8 mm bars with $f_y = 593$ MPa and $E_s = 196$ GPa; 10.0 mm bars with $f_y = 560$ MPa and $E_s = 212$ GPa; and 12.5 mm. In all cases, the spacing between flexural bars were 99 mm. Constructive rebars were used in the bottom face of slabs, made with 6.3 mm bars at spacing of 198 mm in both directions. These rebars were not

submitted to tensile tests once they were not of interest in this research.

Concrete was made with Portland composite cement CP II-Z-32 (with 6 to 14% of pozzolan), natural sand and rolled pebble with a maximum size of 19 mm. The concrete compressive strength was determined with tests on 100 x 200 mm cylinders performed at the same day of tests on slabs. The slabs and the cylindrical concrete specimens were cured with wet covering during 7 days and then they were stored until the day of the tests at ambient weather conditions.

Slabs were supported on two opposite borders and the load was applied upwards by a hydraulic jack in increments of 10 kN. Loading was transmitted in the soffit of the slab by a square steel plate with sides of 85 mm and with thickness of 50 mm. A steel ball joint was used between the steel plate and the jack in order to permit rotations and avoid the transference of moments, especially in cases of asymmetric loading. Reactions were provided by steel beams anchored to a strong floor by high strength steel rods. A load cell placed between the jack and the ball joint was used to measure the loading increments. At each load step, intervals of 5 minutes were made in order to inspect the slabs' cracking and to measure displacements and strains on concrete and on flexural rebars. Figure 3 and Table 1 presents the geometric characteristics of the slabs.

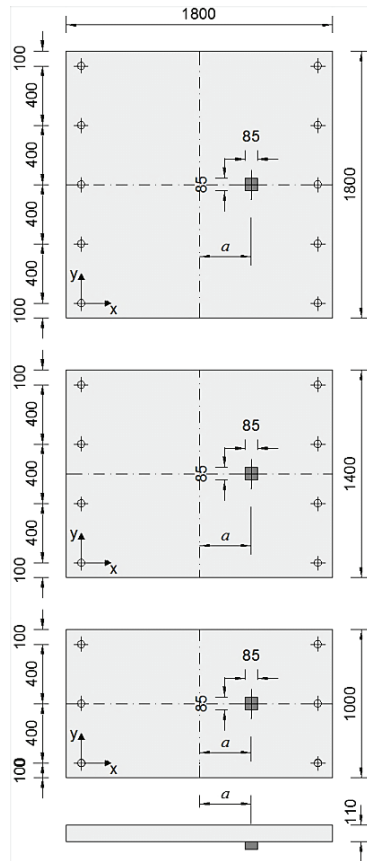


Figure 3. Geometric characteristics of the slabs.

Recommendations from ACI 318

ACI states that the shear strength of slabs near columns or concentrated loads is governed by the more severe of two conditions: beam action, where the critical section to be investigated extends in a plane across the entire slab width (see Equation 1 and Figure 4a); two-way action, where the critical perimeter to be investigated is assumed to be $d/2$ from the column faces (see Equation 2 and Figure 4b).

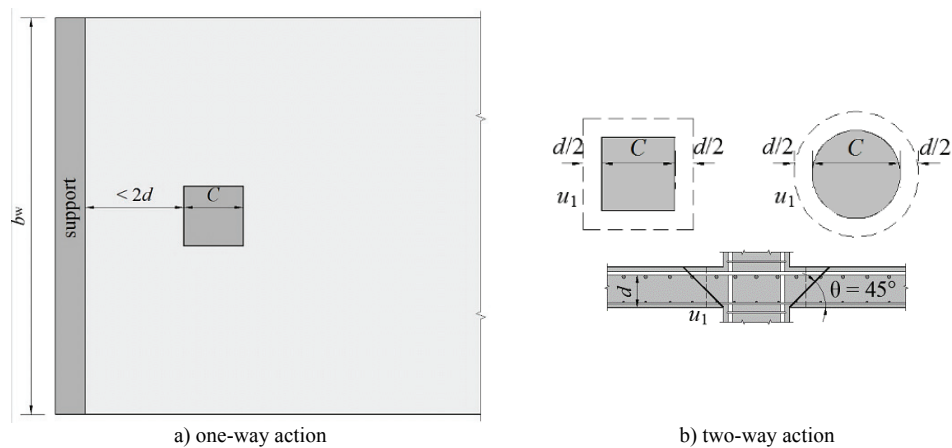


Figure 4. Control perimeter according to ACI 318.

Table 1. Characteristics of tested slabs.

Slab	b_w (mm)	e_r (mm)		H (mm)	d (mm)	ρ (%)	f_c (MPa)	a (mm)
		x	y					
M-8-0		12.5	8.0	111	88	0.99	42	0
M-10-0		12.5	10.0	112	90	1.22	51	0
M-12-0		12.5	12.5	110	87	1.57	44	0
M-8-267		12.5	8.0	112	89	0.98	42	267
M-10-267		12.5	10.0	111	89	1.23	50	267
M-12-267	1,800	12.5	12.5	110	87	1.57	45	267
M-8-400		12.5	8.0	112	89	0.98	42	400
M-10-400		12.5	10.0	111	89	1.23	49	400
M-12-400		12.5	12.5	110	87	1.57	36	400
M-8-480		12.5	8.0	113	90	0.97	49	480
M-10-480		12.5	10.0	112	90	1.22	58	480
M-12-480		12.5	12.5	110	87	1.57	45	480
P-8-0		12.5	8.0	123	100	0.87	44	0
P-8-267	1,000	12.5	8.0	118	95	0.92	44	267
P-8-400		12.5	8.0	118	95	0.92	44	400
V-8-0		12.5	8.0	118	95	0.92	45	0
V-8-267	1,400	12.5	8.0	133	110	0.79	45	267
V-8-400		12.5	8.0	128	105	0.83	45	400

$$V_{R,c} = 0.17 \cdot \sqrt{f_c} \cdot b_w \cdot d \quad (1)$$

$$V_{R,c} = 0.33 \cdot \sqrt{f_c} \cdot u_1 \cdot d \quad (2)$$

where: f_c (in MPa) is the compressive strength of concrete limited to 69 MPa; b_w (in mm) is the slab width used to estimate the punching strength in cases of one-way action; u_1 (in mm) is the length of a control perimeter as show in Figure 4b; d (in mm) is the effective depth of the slab.

Recommendations from Eurocode 2

Eurocode 2 states that the punching strength of slabs without shear reinforcement shall be checked using Equation 3. EC2 does not present any explicit recommendation to check the shear resistance of flat slabs for one-way action, but if necessary, the designer may use Equation 3 and replace u_1 per b_w . Figure 5 shows the control perimeter for use in Equation 3.

$$V_{R,c} = 0.18 \cdot k \cdot (100 \cdot \rho \cdot f_c)^{1/3} \cdot u_1 \cdot d \quad (3)$$

$$k = 1 + \sqrt{\frac{200}{d}} \leq 2.0 \quad (4)$$

where: f_c is in MPa and is limited to 90 MPa; k is the size effect obtained using Equation 4; ρ is the geometric flexural reinforcement ratio calculated as and limited to a maximum of 0.02; ρ_x and ρ_y are the ratios of flexural reinforcement in orthogonal directions determined for widths equal to the side of the column plus $6 \cdot d$ ($3 \cdot d$ to either side).

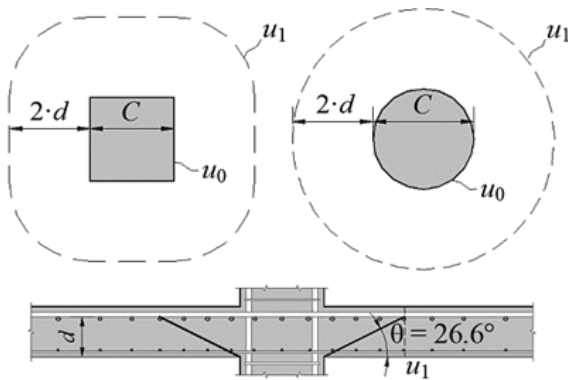


Figure 5. Control perimeter according to Eurocode 2.

Flexural resistance

The flexural resistance of tested slabs may be checked using yield lines theory. In case of one-way slabs, the ultimate flexural resistance is the load (V_{flex}) for which a collapse mechanism characterized by a linear plastic hinge spreads through the whole width of the slab. This may be calculated using Equations 5 and 6.

$$m_u = A_{s,x} \cdot f_{ys} \cdot d^2 \left(1 - \frac{\rho \cdot f_{ys}}{2 \cdot f_c} \right) \quad (5)$$

$$V_{flex} = \frac{(L-c) \cdot b_w \cdot m_u}{\left(\frac{L+2a-c}{2} \right) \cdot \left(\frac{L-2a-c}{2} \right)} \quad (6)$$

where: m_u is the ultimate moment of resistance per unit width; $A_{s,x}$ is the area of flexural reinforcement in the longitudinal direction; f_{ys} is the yield stress of reinforcement; L is the effective span of the slab; c is the length of the side of the loaded area; a is the distance from the loading point to the center of the slab.

Results and discussion

Vertical displacements

Figure 6 presents the profile of vertical displacements in the longitudinal direction for

slabs M-8-0 to M-8-480, from the early to the final loading stages in which they were measured. It illustrates in general the load-displacement response of tested slabs as the loading points moved towards the supports. Slabs with symmetric load presented an almost linear variation of displacements along the span since beginning until the end of tests.

As the loading points moved towards the supports, the shape of the deflected profiles of slabs changed, assuming a slightly concave geometry, showing a non-linear variation of displacements along the slabs radius. This was especially observed for slabs with higher values of a (400 and 480 mm), in which the profile of vertical displacements indicates that the slabs' zone between the loading point and the closer support is submitted to high rotations, which may possibly increase shear strains in this side of the slab.

In the case of type M slabs, it was observed a greater variation in vertical displacements along the transverse direction for cases where the load was applied asymmetrically. In these cases, the displacements measured at the edges of the slabs was around 5 to 6 times smaller than the displacement measured at the point of load application, while it was around half of this value for slabs loaded symmetrically. For the case of slabs with reduced width (types P and V) it was possible to notice a response in terms of transversal displacements similar to what is expected for wide beams, especially for slabs type P, in which small variations were observed between slabs center to its borders. Figure 7 presents load-displacement curves for tested slabs as a function of the loading position (a) showing that both transversal flexural reinforcement ratio and slabs' width influence significantly the load-displacement response. These curves also show that the deflection in the ultimate load stage reduced from 25 to 50% as the load approached the supports.

Strains on concrete surface

Only tangential strains were measured for all tested slabs. This decision was taken considering that there is strong experimental evidence (see Oliveira, Melo, & Regan (2000) (5) and Ferreira, Melo, Regan, & Vollum (2014) (6) among others) showing that they are more relevant for slab-column connections. Tangential strains were measured by a pair of strain gauges placed in the bottom surface of slabs. They were placed on opposite sides of the loading plate, at distances of 45 mm from its edges.

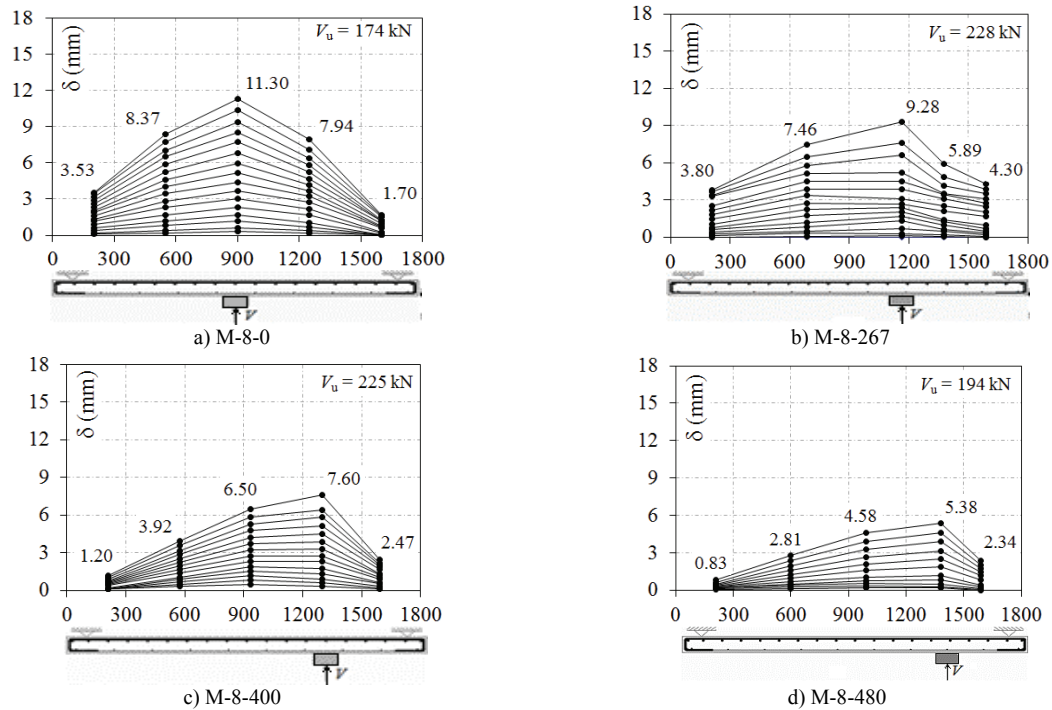


Figure 6. Profile of vertical displacements in the longitudinal direction of slabs M-8-0 to M-8-480.

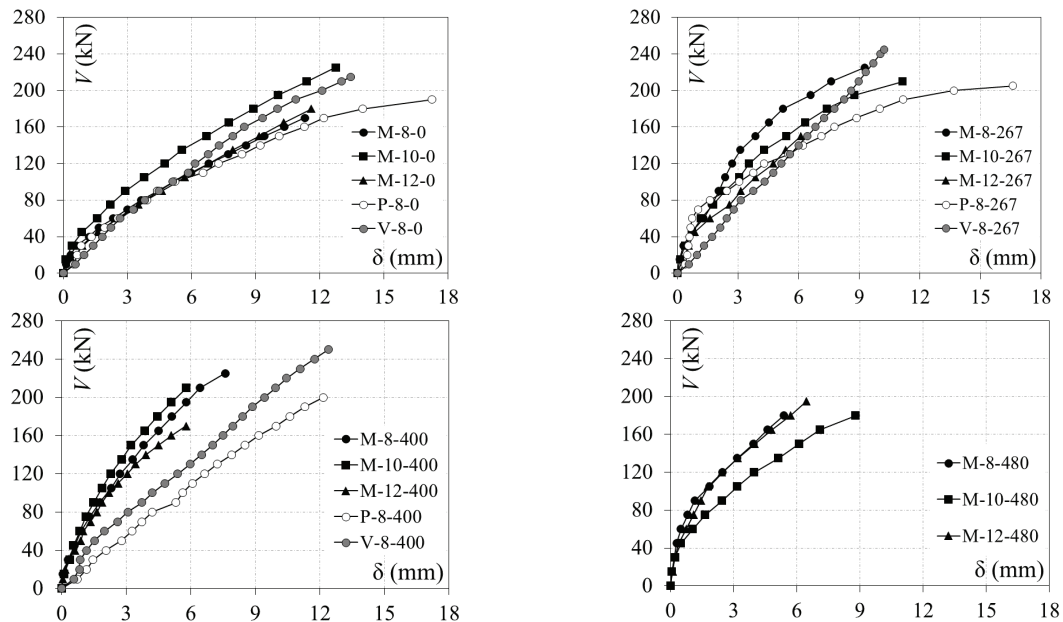


Figure 7. Load-displacement curves.

For cases of symmetric load, Ec1 and Ec2 were placed at equal distances from the slabs' center. Nevertheless, for cases of asymmetric load, Ec1 was placed between the load plate and the closer support and Ec2 was placed between the load plate and the slabs' central axle. For cases of slabs type M and V, flexural compression was far from being a limiting state. However, even without results of longitudinal strains, it can be concluded

that for slabs type P it may be a relevant failure mode that should be checked in similar design cases, being clearly the failure mode of slab P-8-0, as show in Figure 8.

Figure 9 presents strains on concrete for slabs M-8-0, M-8-267 and M-8-400, as an illustration of observed results for slabs type M. In general, results show that strains increased as loads were closer to supports, contrasting with the fact that

stresses caused by flexure should reduce. Results also indicate significant differences on strains measured by the opposite gauges for asymmetric load, varying between 23, 64 and 95%, indicating that the part of the slab between the loaded plate and the closer support is submitted to larger rotations. However, this seems to be a behavior restricted to a small area around the loaded area that influences tangential strains on concrete and possibly shear strains in the longitudinal direction.

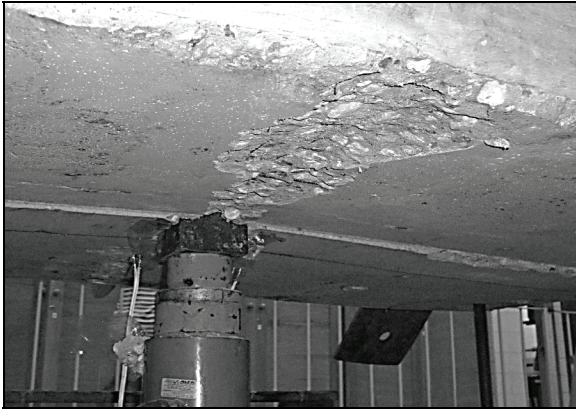


Figure 8. Slab P-8-0 after failure.

Strains on flexural reinforcement

Strains on flexural rebars were measured with pairs of strain gauges placed on opposite sides of bars. Figure 10 present profiles of strains on flexural reinforcement for slabs M-8-0 and M-8-400 and for slabs M-12-0 and M-12-400.

In general, for slabs type M, punching failures occurred with little or no yielding of flexural reinforcement bars. For slabs type P and V, rebars within distances of $2 \cdot d$ to $3 \cdot d$ from the loaded plate yielded before failure. The transversal

flexural reinforcement ratio seems to influence in the stress distribution after cracking. Figure 10 shows that for slabs with smaller ratios stresses distribution were more sustained along the span of the slabs while in slabs with transverse reinforcement ratio equal to the longitudinal ones the trend was that flexural stresses were more concentrated in a small area around the loaded plate.

Cracking pattern

Figure 11 presents the cracking pattern and the failure surfaces for slabs M-8-0, M-10-0 and M-12-0 and M-8-480, M-10-480 and M-12-480.

The influence of the transversal flexural reinforcement ratio in the stresses distribution on the tested slabs may also be observed through the analysis of their cracking pattern. Slabs with lower transverse flexural reinforcement presented a radial cracking pattern with cracks spreading towards the supports. Furthermore, for the slabs in which the transverse flexural reinforcement ratio was equal to the longitudinal one, cracks were mainly perpendicular to the slabs' span and more concentrated around the loading point.

As the loaded area moved towards the supports, the flexural cracking reduced significantly, leading to brittle punching failures, e.g. slab M-12-480, in which punching shear failure occurred with almost no flexural cracking. The position of the loading point also affected the inclination of the failure surface. Slabs with symmetric loading presented failure surfaces inclined of 24° . For slabs with asymmetric loading the failure surface was steeper for the region between the load and the closer support, reaching a maximum of 67° for slab M-12-480.

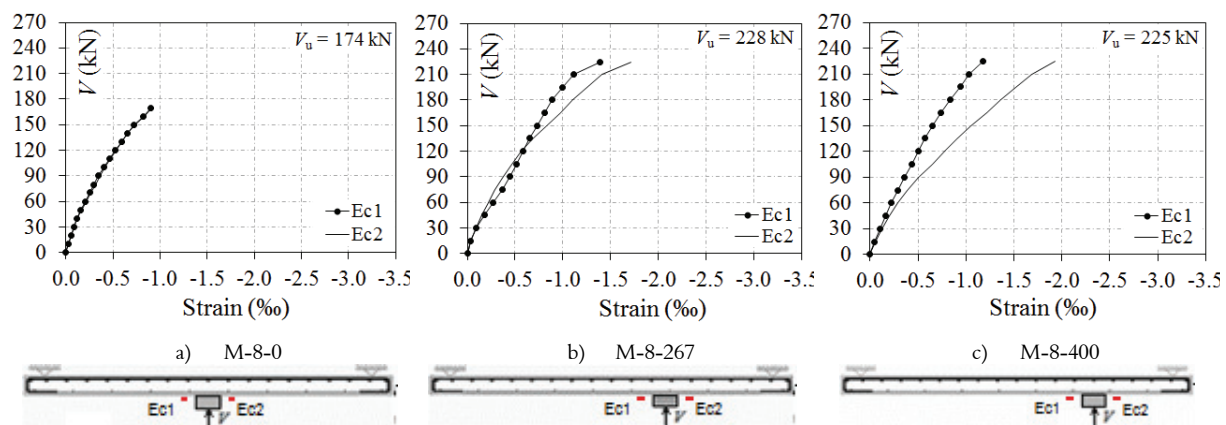


Figure 9. Strains of concrete at the soffits of tested slabs.

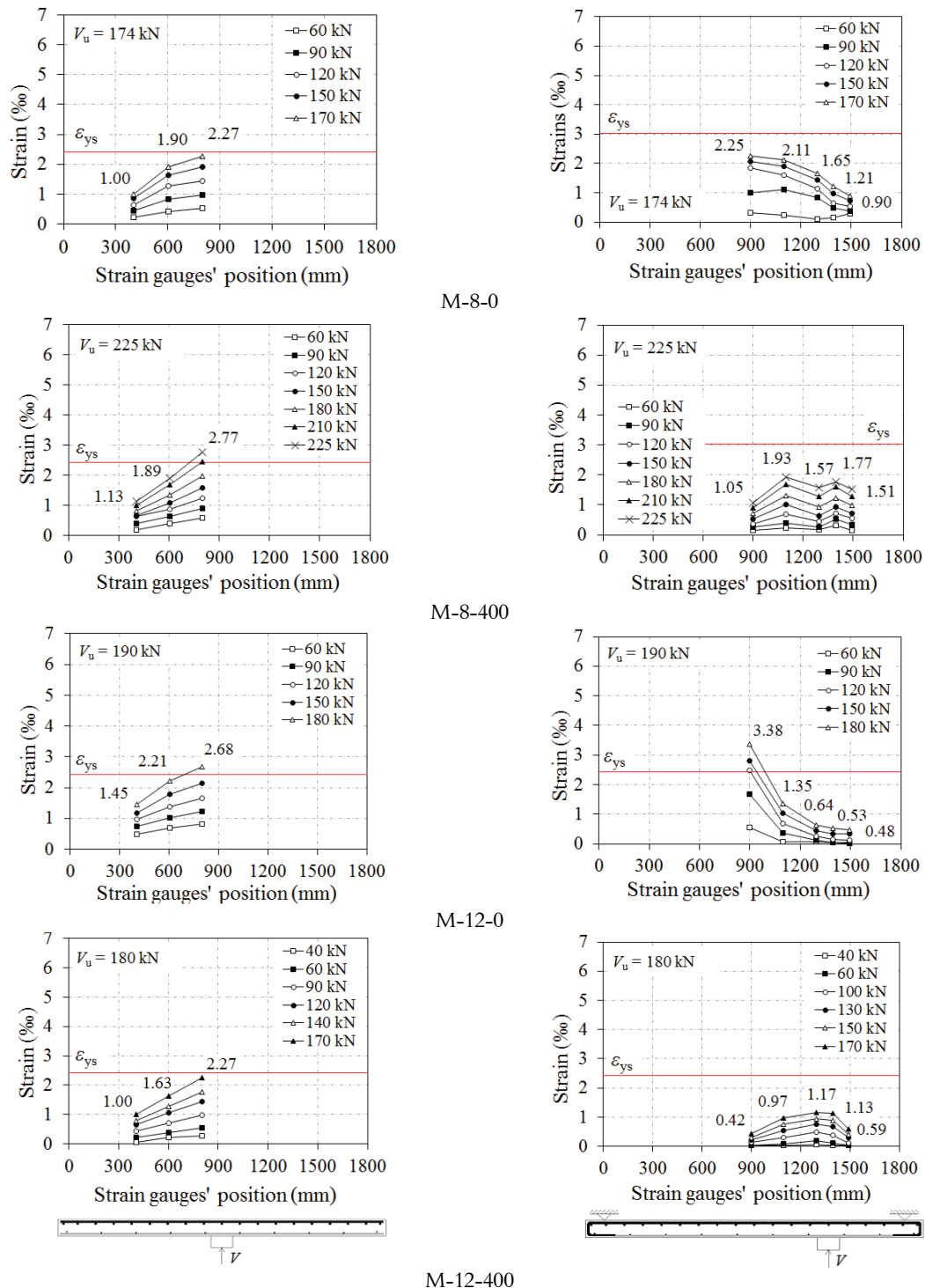


Figure 10. Profile of strains on flexural reinforcement for slabs M-8-0, M-8-400, M-12-0 and M-12-400.

Ultimate loads and failure modes

Table 2 presents the ultimate loads and the failure modes of tested slabs. All type M slabs failed by punching. For slabs with smaller breadths (types P and V), flexure had a greater influence on the observed results. Almost all these slabs presented ductile failures, with many of the monitored bars

yielding before failure. Slab P-8-0 failed clearly by flexure, as commented previously and show in Figure 8. Except for slabs V-8-267 and V-8-400, which failed abruptly by punching shear, all others were close to fail by flexure when suddenly the punching failure mechanism occurred. None of tested slabs failed by shear as in wide beams.

Comparison of tests results with predictions by codes of practice

Table 3 and Figure 12 show comparisons between experimental results obtained in tests and theoretical resistances predicted by ACI and EC2. ACI presented reliable and safe predictions, though relatively

conservative. Although EC2 presented average results closer to those observed in tests, in two of the eighteen tested slabs, it estimated that the ultimate resistance would be greater than it was experimentally observed. In both cases, this happened to type M slabs, which had width of 1,800 mm.

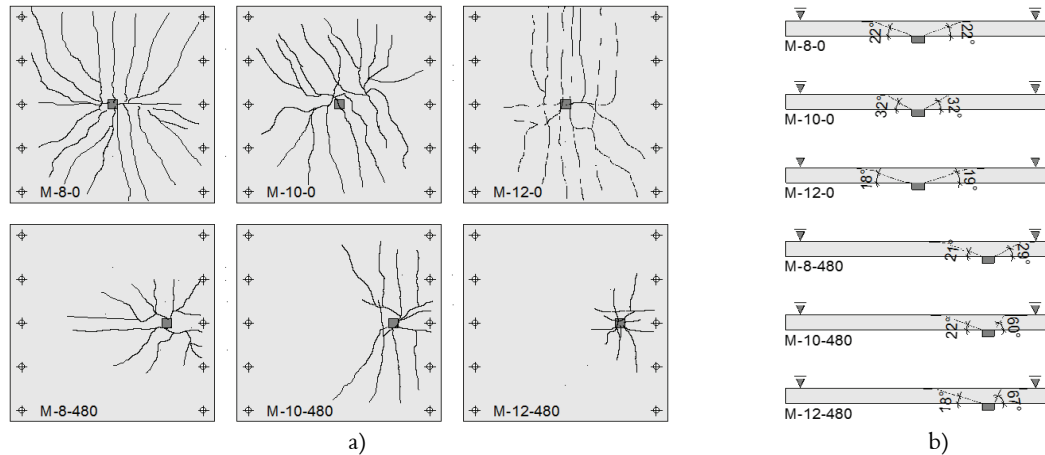


Figure 11. Cracking pattern and failure surface of slabs.

Table 2. Ultimate loads and failure modes.

Slab	b_w (mm)	h (mm)	d (mm)	ρ (%)	f_c (MPa)	a (mm)	V_u (kN)	V_{flex} (kN)	V_u / V_{flex}	Failure Mode
M-8-0	1,800	111	88	0.99	42	0	174	267	0.65	P
M-10-0		112	90	1.22	51	0	232	273	0.85	P
M-12-0		110	87	1.57	44	0	190	269	0.71	P
M-8-267		112	89	0.98	42	267	228	305	0.75	P
M-10-267		111	89	1.23	50	267	211	311	0.68	P
M-12-267		110	87	1.57	45	267	160	308	0.52	P
M-8-400		112	89	0.98	42	400	225	371	0.61	P
M-10-400		111	89	1.23	49	400	215	377	0.57	P
M-12-400		110	87	1.57	36	400	180	364	0.49	P
M-8-480		113	90	0.97	49	480	194	454	0.43	P
M-10-480		112	90	1.22	58	480	191	460	0.41	P
M-12-480		110	87	1.57	45	480	206	450	0.46	P
P-8-0	1,000	123	100	0.87	44	0	205	149	1.37	F
P-8-267		118	95	0.92	44	267	204	170	1.20	FP
P-8-400		118	95	0.92	44	400	202	207	0.98	FP
V-8-0	1,400	118	95	0.92	45	0	222	210	1.06	FP
V-8-267		133	110	0.79	45	267	250	239	1.04	FP
V-8-400		128	105	0.83	45	400	256	291	0.88	P

Note: P: punching shear failure; F: flexural failure; FP: Flexural-punching shear failure.

Table 3. Ultimate loads and failure modes.

Slab	d (mm)	ρ (%)	f_c (MPa)	V_u (kN)	FM	ACI				EC2			
						V_{wb} (kN)	V_{rs} (kN)	V_u / V_{calc}	FM	V_{wb} (kN)	V_{rs} (kN)	V_u / V_{calc}	FM
M-8-0	88	0.99	42	174	P	350	131	1.33	P	396	159	1.09	P
M-10-0	90	1.22	51	232	P	392	148	1.57	P	460	187	1.24	P
M-12-0	87	1.57	44	190	P	353	131	1.45	P	463	184	1.03	P
M-8-267	89	0.98	42	228	P	265	133	1.72	P	299	162	1.41	P
M-10-267	89	1.23	50	211	P	288	144	1.47	P	340	183	1.15	P
M-12-267	87	1.57	45	160	P	268	133	1.20	P	349	186	0.86	P
M-8-400	89	0.98	42	225	P	236	133	1.69	P	266	162	1.39	P
M-10-400	89	1.23	49	215	P	253	142	1.51	P	300	182	1.18	P
M-12-400	87	1.57	36	180	P	213	119	1.51	P	288	172	1.04	P
M-8-480	90	0.97	49	194	P	241	146	1.33	P	264	173	1.12	P
M-10-480	90	1.22	58	191	P	261	157	1.21	P	300	196	0.98	P
M-12-480	87	1.57	45	206	P	223	133	1.55	P	291	186	1.11	P
P-8-0	100	0.87	44	205	F	226	162	1.26	P	243	194	1.06	P
P-8-267	95	0.92	44	204	FP	161	150	1.36	P	176	180	1.16	P _{wb}
P-8-400	95	0.92	44	202	FP	143	150	1.41	P _{wb}	157	180	1.29	P _{wb}
V-8-0	95	0.92	45	222	FP	304	152	1.46	P	331	182	1.22	P
V-8-267	110	0.79	45	250	FP	264	190	1.31	P	274	225	1.11	P
V-8-400	105	0.83	45	256	P	224	177	1.45	P	236	210	1.22	P
Average						1.43			Average			1.15	
COV						0.10			COV			0.12	

Note: P: punching shear failure; F: flexural failure; FP: Flexural-punching shear failure; P_{wb}: one-way shear failure.

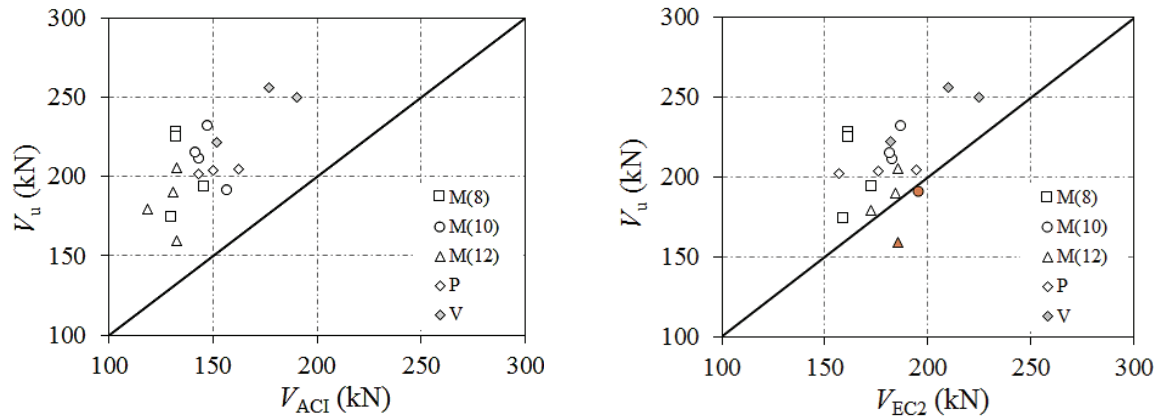


Figure 12. Comparison between experimental strengths and codes predictions.

Regarding one-way shear resistance, it was expected that this would be the failure mode at least for slab P-8-400, which actually turned out not being observed in the carried tests. This slabs actually failed by punching shear with ultimate resistance 30 to 40% higher than the estimated one-way shear (wide beam) resistance, indicating that the provisions presented by codes for the case of slabs may be over conservative.

Conclusion

One-way slabs submitted to asymmetric concentrated loads is a situation for which there is very little experimental evidence available, thus being difficult to provide definitive conclusions. In the light of these tests' results, it is possible to draw the following conclusions:

Design provisions presented by ACI and EC2 to estimate one-way shear resistance of one-way reinforced concrete slabs under concentrated loads are safe although relatively conservative.

For punching shear, ACI provisions were in general over conservative while EC2 provided more accurate strength predictions, with 10% unsafe results.

The series of testes presented in this paper showed that, before failure, significant stress redistribution occur due to bending, enabling shear softening in the parts of the slab with higher elastic stresses. This was also pointed by Sagaseta et al. (2011).

In the failure load stage, it seems appropriate, for strength predictions, the assumption of a constant average stress around control perimeters, as considered by ACI and EC2, although failure surface in tests where the load was close to the support were asymmetrical.

The use of additional steel in the transversal direction does not provide significant gains of ductility and of resistance, as observed in tests.

This paper shows that more tests are necessary in order to draw definitive conclusions about this topic. It would be important to provide a significant number of results for one-way and two-way slabs submitted to asymmetric point loads.

It would be also important to have results for thicker slabs, with total height equal or above 200 mm, in order to represent cases of slabs in natural scale and to check size effect for these types of shear failures.

Acknowledgements

The authors are grateful to the Brazilian research funding agencies CAPES (Higher Education Coordination Agency), CNPq (National Council for Scientific and Technological Development) and FAPESP (Para Research Foundation). They also would like to express their gratitude to Professor Paul E. Regan for his support and advices throughout this research.

References

- American Concrete Institute (ACI). (2014). *Building Code Requirements for Structural Concrete (ACI 318-11) and Commentary*. Farmington Hills, MI: American Concrete Institute.
- Comité Européen de Normalisation (CEN). (2005). *EN 1992-1-1 Eurocode 2 - design of concrete structures: part 1-1. General rules and rules for buildings*. Brussels, BEL: Comité Européen de Normalisation.
- Ferreira, M. P., Melo, G. S., Regan, P. E., & Vollum, R. L. (2014). Punching of reinforced concrete flat slabs with double-headed shear reinforcement. *ACI Structural Journal*, 111(2), 1-12.
- Forsell, C., & Holmberg, A. (1946). Concentrated load on concrete slabs. *Betong*, 31(2), 95-123.
- Lantsoght, E. O. L., van der Veen, C., & Walraven, J. C. (2013). Shear in one-way slabs under concentrated load close to support. *ACI Structural Journal*, 110(2), 275-284.

- Oliveira, D. R., Melo, G. S., & Regan, P. E. (2000). Punching strength of flat plates with vertical or inclined stirrups. *ACI Structural Journal*, 97(3), 485-491.
- Regan, P. E., & Rezai-Jorabi, H. (1988). Shear resistance of one-way slabs under concentrated loads. *ACI Structural Journal*, 85(2), 150-157.
- Sagaseta J., Muttoni A., Fernández Ruiz M., & Tassinari, L. (2011). Non-axis-symmetrical punching shear around internal columns of RC slabs without

transverse reinforcement. *Magazine of Concrete Research*, 63(6), 441-457.

Received on April 7, 2015.

Accepted on September 14, 2015.

License information: This is an open-access article distributed under the terms of the Creative Commons Attribution License, which permits unrestricted use, distribution, and reproduction in any medium, provided the original work is properly cited.